

DISTORTED IMAGE RESTORATION USING STACKED ADVERSARIAL NETWORKS

Yi Gu[†] Yuting Gao[‡] Jie Li^{†*} Chentao Wu[†] Weijia Jia[§]

[†] Department of Computer Science and Engineering, Shanghai Jiao Tong University, China

[‡] Department of Electrical and Computer Engineering, Texas A&M University, US

[§] Institute of Artificial Intelligence and Future Networks, Beijing Normal University & UIC, China

ABSTRACT

Liquify is a common technique for distortion. Due to the uncertainty in the distortion variation, restoring distorted images caused by liquify filter is a challenging task. Unlike existing methods mainly designed for specific single deformation, this paper aims at automatic distorted image restoration, which is characterized by seeking the appropriate warping of multi-type and multi-scale distorted images. In this work, we propose a stacked adversarial framework with a novel coherent skip connection to directly predict the reconstruction mappings and represent high-dimensional feature. Since there is no available benchmark which hinders the exploration, we contribute a distorted face dataset by reconstructing distortion mappings based on CelebA dataset. We also introduce a novel method for generating synthesized data. We evaluate our method on proposed benchmark quantitatively and qualitatively, and apply it to the real world for validation.

Index Terms— Distorted Image Restoration, Liquify, Benchmark, Adversarial Framework

1. INTRODUCTION

Liquify [1] is significantly valued to the applications in image editing. As shown in Figure 1, the liquify filter can be used to distort the image to achieve various special effects, such as concave lens, convex lens, distorting mirror, etc. Although we can use the image editing application to liquify the image, it is difficult to restore the distorted image, which takes the programmer much time to remove special effects by liquify operation. To this end, we expect an automatic distorted image restoration method. Users only need to upload a distorted image, and they will get the rough original image back.

In this paper, the distorted image restoration task we are discussing is a relative novel work. Previous efforts mainly focus on specific single deformation. One common practice [2, 3, 4, 5] is to rely on additional information acquired by the sensor to reconstruct the 3D distortion shape. The other is to [6, 7, 8, 9] correct images based on geometric algorithms. However, our task is to achieve distortion restoration

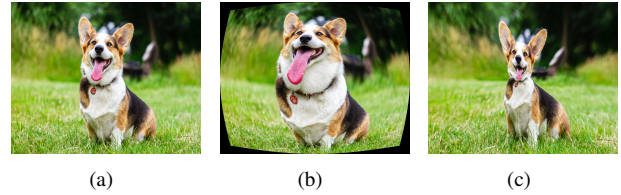


Fig. 1. For a given original image (a), we show the convex lens effect (b) and the concave lens effect (c). Our task is to restore the distorted image to the original one.

for multi-type with multi-scale. Therefore, this task presents two new challenges: 1) Degrees of distortion in image editing are irregular and unnatural. 2) Types of distortion are various and unpredictable. Since it's unrealistic to tackle all cases at a time, in this paper we consider the case of two-type distortion (concave and convex) with multi-scale as an initial study.

Motivated by the success of applying generative adversarial networks [10] in image generation, we present a novel stacked adversarial network to alleviate the above issues. We define the solution as a two-stage process: rectification and refinement. The first stage reconstructs the mapping while the second stage produces high frequency feature. We propose a coherent skip connection which is beneficial in convergence speed and high-quality overall optimum. Since there is no existing dataset available to evaluate this task, we introduce a novel procedure to create synthesized data and release a distorted face dataset which can be used as a benchmark to fill the vacuum.

Our main contributions include: 1) We design a generic stacked framework as a baseline for distorted image restoration task. 2) We propose to add coherent skip connection to construct the correlation of deep deformation features. 3) We contribute a benchmark for this task. To the best of knowledge, it is the first available dataset on this domain. 4) We introduce a novel method to synthesize distortion images.

2. RELATED WORK

Traditional approaches for distorted image restoration include hardware assistance and geometric principle. The former re-

This work has been partially supported by NSFC Grants 61932014, and Research Collaboration Grant from NII, Japan.

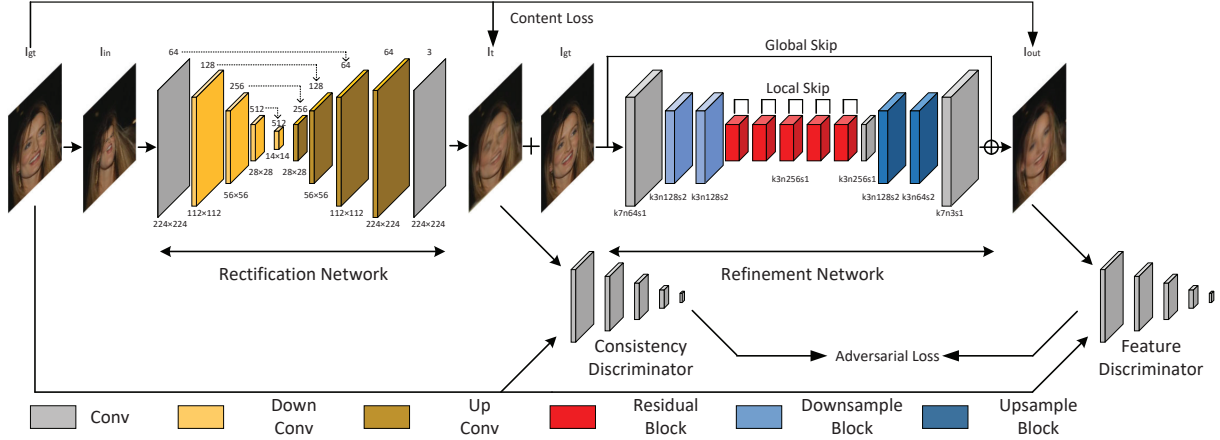


Fig. 2. Framework Overview. The number below the block of rectification network represents the size of feature map and the number above represents the channel. Kernel size (k), channel number (n) and stride (s) are indicated for each block of refinement network. We add the global skip cascaded to the local skip in the refinement network.

lies on the hardware to attain additional information, such as BFS-Auto [2], laser beams [3], cameras [4], depth sensors [5], etc. These efforts use the device to reconstruct 3D shapes. The geometric principle focuses on the geometric correction of curved images. It uses geometric algorithms such as Curvilinear Projection [6], Covariance Matrix Adaptation [7], Low-rank Textures [8], etc. Both approaches are aimed at specific deformation like cylinder [6], barrel[7], grouped circular arcs [9], but in this task there are various irregular distortions caused by liquify, it requires the solution to tackle the complexity and uncertainty of distortion.

Recently, GANs have made great progress in respect of perceived quality. [11, 12, 13] manage to fill the masked or missed regions in images. They use joint training by local and global losses to maintain the content coherence. But our task is a global consistency problem, local generative and discriminative learning is useless. This task not only requires the solution to maintain the overall coherence of the image, but also requires that the generated image is perceptually convincing compared with the original one. Motivated by GAN’s ability in inpainting and reconstruction, we implement the characteristics of GAN to achieve image restoration, especially for distorted image caused by liquify filter.

3. BENCHMARK

Obtaining the required images in the real world is difficult. Thus, we consider to utilize image geometric transformation to batch generate distorted image. We choose CelebA dataset [14] as our basic dataset for modification. This dataset contains a large amount of aligned and cropped face data, which is suitable as the distortion processing object.

Imaging distortion is an image interpolation. We assume the coordinate of a pixel m in the source image I is (u, v) ,

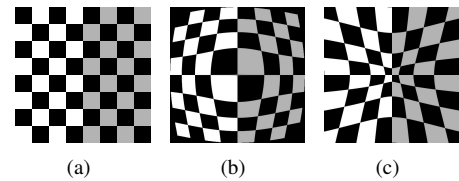


Fig. 3. Image distortion result. From left to right:(a) original image. (b) negative distortion. (c) positive distortion.

and coordinate of pixel m' in the destination image I' is (x, y) [2]. In the paper, we implement distortion in a polar coordinate. Corresponding polar coordinate of pixel m and m' are (r, θ) and (r', θ') , so we can obtain that radius from the center $r = \sqrt{x^2 + y^2}$ and $\theta = \tan^{-1} \frac{y}{x}$. We define the distortion as a forward mapping function from source pixel to destination pixel.

$$\begin{cases} r' = k \cdot r, & \theta' = \theta \\ x' = r' \cdot \cos\theta', & y' = r' \cdot \sin\theta' \end{cases} \quad (1)$$

We call parameter k the scaling factor for parametric mappings. If $k = 1$, the processed image stays the same as the original one. If $0 < k < 1$, it performs convex distortion pixels within the selected region takes the value from pixels. If $k > 1$, it performs concave distortion where magnification increases with the distance from the center. Finally we convert the polar coordinate into Cartesian coordinate and get the distorted image. Figure 3 illustrates our distortion result.

We create the dataset consisting of 100,000 negative distortion images and 102,599 positive images. Parameter k for negative and positive distortion take value 0.5, 0.8 and 1.5, 2.7 separately. We should notice that since the distorted image itself is unnatural, our data does not need to be augmented to reduce the gap between real and synthetic data.

Table 1. Quantitative evaluations in terms of PSNR and SSIM at the overall benchmark S0 and four different categories of distortion S1-S4, which correspond to four distortion parameters at 0.5, 0.8, 1.5 and 2.7, respectively. Higher values are better.

	PSNR					SSIM				
	S0	S1	S2	S3	S4	S0	S1	S2	S3	S4
Our method	25.12	23.57	26.42	25.99	24.49	0.813	0.782	0.856	0.834	0.779
Rectification Network	21.42	19.43	24.33	22.37	19.54	0.773	0.731	0.839	0.802	0.721
Refinement Network	17.36	16.82	17.99	17.62	17.01	0.544	0.542	0.563	0.544	0.528
Refinement w/o \mathcal{L}_{adv}	17.17	16.96	17.78	17.41	16.52	0.730	0.706	0.764	0.751	0.701
Refinement w/o \mathcal{L}_{mse}	5.49	-	-	-	-	0.072	-	-	-	-
Rectification w/o \mathcal{L}_{adv}	18.93	18.01	19.77	19.27	18.68	0.742	0.711	0.789	0.763	0.706
Rectification w/o \mathcal{L}_{mse}	6.83	-	-	-	-	0.061	-	-	-	-

4. METHOD

4.1. Rectification Network

As shown in Figure 2, training is an adversarial process introduced by [10] in each step, where the generator competes with the discriminator and the two networks are optimized alternately. The purpose of rectification network is to learn a non-linear transformation from warped space to normal space. We follow the architectural guidelines of U-Net [15] due to its effectiveness in the semantic segmentation.

However, U-Net is based on fully convolutional networks and it is designed for pixel-wise prediction. But our task is a global consistency problem, it requires a soft optimum. So we modify the architecture that our feature map is down sampled to 512 channels for shallow features and each upsampling step consists of an upsampling layer doubling the size of feature map and two repeated 3×3 convolution layers yielding the number of feature channel at 1/4 scale. We also modify the padding scheme of each convolution layer to keep the input and output the same size.

4.2. Refinement Network

Since cascaded architecture has verified the effectiveness of image generation [17], we design a refinement network to produce high frequency details and preserve overall consistency. It is made up of three convolution layers, two down-sample blocks, five residual blocks [18] and two upsample blocks. Each downsample block is composed of a 3×3 convolution layer, a BN layer and a PReLU activation. It doubles the number of feature channel while yielding the feature map at 1/2 scale. Each upsample block consists of a 3×3 deconvolution layer, a BN layer and a PReLU activation. It halves the feature channel number.

We propose a coherent skip connection mechanism to make the model generalize better and train faster. We add a local skip connection in each residual block to capture finer details from local receptive fields, and a global skip connection between corresponding layers to pass details from bottom layers to top layers. These skip connections show that they help recover full spatial resolution on network output.

4.3. Discrimination Network

Distorted image restoration is a global consistency task, which requires the generated content to be consistent with the surrounding contexts. Therefore, we adopt the global discriminator where the architecture is the same as [16] to keep the whole image perceptually consistent.

4.4. Loss

We adopt the content loss \mathcal{L}_{mse} and adversarial loss \mathcal{L}_{adv} from some GAN approaches [19] [20] to optimize the generator network. \mathcal{L}_{mse} is utilized to restore general content while \mathcal{L}_{adv} focuses on completing texture details. The overall loss function can be formulated as:

$$\mathcal{L} = \mathcal{L}_{mse} + \lambda \mathcal{L}_{adv}. \quad (2)$$

where λ is the trade-off weight set by the cross validation experiments. The discriminator of each step shares the same formulation of the loss function.

5. EXPERIMENT

We evaluate our method on proposed benchmark through qualitative and quantitative analysis. We rely on visual perception for qualitative evaluation and adopt peak signal to noise ratio (PSNR) and structural similarity (SSIM) for quantitative evaluation. We also apply our model to the real world for validation.

Qualitative results. Figure 4 shows our restoration results on the benchmark. The results in the third column of each panel in the figure show that our model obtains the perceptually convincing images which artially or completely supplement the missing details and has good generalization ability on a variety of distorted images.

Quantitative results. In order to further explore the relationship between deep deformation features, we report our quantitative evaluation on the benchmark in terms of PSNR and SSIM, as shown in Tables 1. The results show that our model illustrates good generalization on whether positive or



Fig. 4. Benchmark results (a)(b). In each panel from left to right: distorted image, original image and our method result. Application results (c). From left to right: distorted image, original image and restoration image. From top to bottom: concave with arbitrary rate, convex with arbitrary rate, a mixture of convex and concave.

negative distorted images. But as the degree of distortion increases, the restoration performance of our model decreases in both metrics. We then compare our model with the single rectification network and the single refinement network. We can conclude that our method performs better than others and achieves the highest numerical performance. This is due to the nature of our method, which can seek a suitable nonlinear mapping for reconstruction and correct the image by coherent skip connection for corresponding supplement.

Effect of Refinement. We purely rely on the rectification network to produce the image and Table 1 shows the quantitative results. It demonstrates that the refinement network can further optimize the perceptual quality. It helps denoise predictions and produce more details in color and contrast. Besides, by implementing coherent skip connection, the results are more coherent with the target compared with training without the rectification network.

Effect of Rectification. We omit the rectification network and Table 1 shows that only Refinement Network training acquires the lowest numerical performance in two metrics. We can conclude that utilizing more reconstruction term can result in partly restoration for distorted image but does not guarantee the overall image content is correct.

Effect of Loss. We investigate the effectiveness of the loss function in the two stages. As shown in Table 1, without the content loss to guide the optimization, the results are completely incorrect. And without the adversarial loss, the two metrics are lower than those of training with the adversarial loss. The two loss functions serve as an inpainting term

for restoration, which is beneficial to capture the structure and encourages the network to produce sharp content.

Application. We find some pictures from the Pexel website for real world validation. Figure 4 shows several interesting restoration examples. Since the deep learning model is data-driven and our dataset only has concave and convex distortions, our model cannot generalize on other special effects. But the generalization of our method we have verified demonstrates that if sufficient training data is provided, the model is able to generalize on other types of distortions.

Limitation. Some limitations still exist. One area is that our method doesn't restore the full perceptual distortion and the result still lacks high-frequency details, but it can be handled by user interaction with image editing software. The other area is that the data-driven model is required to continuously learn the input feature so that the model can generalize and restore on unknown distortions. This inspires us to focus on continual learning models in the future.

6. CONCLUSION

As the front work of distorted image restoration, we propose a stacked adversarial framework to directly predict the mapping and produce high frequency feature. We design a coherent skip connection mechanism for local and global optimum. Furthermore, we introduce a novel algorithm to generate synthetic data and contribute the first benchmark in this domain. Experimental results and real world application demonstrate the effectiveness and efficiency of our method.

7. REFERENCES

- [1] Gavin Cromhout, Josh Fallon, Nathan Flood, Katy Freer, Jim Hannah, Francine Spiegel, Pete Walsh, and James Widegren, “Liquifying faces,” in *Photoshop Elements 2 Face Makeovers*, pp. 135–152. Springer, 2003.
- [2] Masahiro Hirano, Yoshihiro Watanabe, and Masatoshi Ishikawa, “3d rectification of distorted document image based on tiled rectangle fragments,” in *2014 IEEE International Conference on Image Processing (ICIP)*. IEEE, 2014, pp. 2604–2608.
- [3] Gaofeng Meng, Ying Wang, Shenquan Qu, Shiming Xiang, and Chunhong Pan, “Active flattening of curved document images via two structured beams,” in *Proceedings of the IEEE Conference on Computer Vision and Pattern Recognition*, 2014, pp. 3890–3897.
- [4] Michael S Brown and W Brent Seales, “Document restoration using 3d shape: a general deskewing algorithm for arbitrarily warped documents,” in *Proceedings Eighth IEEE International Conference on Computer Vision. ICCV 2001*. IEEE, 2001, vol. 2, pp. 367–374.
- [5] Li Zhang, Yu Zhang, and Chew Tan, “An improved physically-based method for geometric restoration of distorted document images,” *IEEE Transactions on Pattern Analysis and Machine Intelligence*, vol. 30, no. 4, pp. 728–734, 2008.
- [6] Gaofeng Meng, Yuanqi Su, Ying Wu, Shiming Xiang, and Chunhong Pan, “Exploiting vector fields for geometric rectification of distorted document images,” in *Proceedings of the European Conference on Computer Vision (ECCV)*, 2018, pp. 172–187.
- [7] Jaroslav Moravec and Miloslav Hub, “Automatic correction of barrel distorted images using a cascaded evolutionary estimator,” *Information Sciences*, vol. 366, pp. 70–98, 2016.
- [8] Linwei Yue, Hongjie Li, and Xianwei Zheng, “Distorted building image matching with automatic viewpoint rectification and fusion,” *Sensors*, vol. 19, no. 23, pp. 5205, 2019.
- [9] Mi Zhang, Xiangyun Hu, Jian Yao, Like Zhao, Jiancheng Li, and Jianya Gong, “Line-based geometric consensus rectification and calibration from single distorted manhattan image,” *IEEE Access*, vol. 7, pp. 156400–156412, 2019.
- [10] Ian Goodfellow, Jean Pouget-Abadie, Mehdi Mirza, Bing Xu, David Warde-Farley, Sherjil Ozair, Aaron Courville, and Yoshua Bengio, “Generative adversarial nets,” in *Advances in neural information processing systems*, 2014, pp. 2672–2680.
- [11] Chao Yang, Xin Lu, Zhe Lin, Eli Shechtman, Oliver Wang, and Hao Li, “High-resolution image inpainting using multi-scale neural patch synthesis,” in *Proceedings of the IEEE Conference on Computer Vision and Pattern Recognition*, 2017, pp. 6721–6729.
- [12] Jiahui Yu, Zhe Lin, Jimei Yang, Xiaohui Shen, Xin Lu, and Thomas S Huang, “Generative image inpainting with contextual attention,” in *Proceedings of the IEEE conference on computer vision and pattern recognition*, 2018, pp. 5505–5514.
- [13] Yijun Li, Sifei Liu, Jimei Yang, and Ming-Hsuan Yang, “Generative face completion,” in *Proceedings of the IEEE Conference on Computer Vision and Pattern Recognition*, 2017, pp. 3911–3919.
- [14] Ziwei Liu, Ping Luo, Xiaogang Wang, and Xiaoou Tang, “Deep learning face attributes in the wild,” in *Proceedings of International Conference on Computer Vision (ICCV)*, December 2015.
- [15] Olaf Ronneberger, Philipp Fischer, and Thomas Brox, “U-net: Convolutional networks for biomedical image segmentation,” in *International Conference on Medical image computing and computer-assisted intervention*. Springer, 2015, pp. 234–241.
- [16] Christian Ledig, Lucas Theis, Ferenc Huszár, Jose Caballero, Andrew Cunningham, Alejandro Acosta, Andrew Aitken, Alykhan Tejani, Johannes Totz, Zehan Wang, et al., “Photo-realistic single image super-resolution using a generative adversarial network,” in *Proceedings of the IEEE conference on computer vision and pattern recognition*, 2017, pp. 4681–4690.
- [17] Qifeng Chen and Vladlen Koltun, “Photographic image synthesis with cascaded refinement networks,” in *Proceedings of the IEEE international conference on computer vision*, 2017, pp. 1511–1520.
- [18] Kaiming He, Xiangyu Zhang, Shaoqing Ren, and Jian Sun, “Deep residual learning for image recognition,” in *Proceedings of the IEEE conference on computer vision and pattern recognition*, 2016, pp. 770–778.
- [19] Yancheng Bai, Yongqiang Zhang, Mingli Ding, and Bernard Ghanem, “Finding tiny faces in the wild with generative adversarial network,” in *Proceedings of the IEEE conference on computer vision and pattern recognition*, 2018, pp. 21–30.
- [20] Phillip Isola, Jun-Yan Zhu, Tinghui Zhou, and Alexei A Efros, “Image-to-image translation with conditional adversarial networks,” in *Proceedings of the IEEE conference on computer vision and pattern recognition*, 2017, pp. 1125–1134.